Soft Matter



View Article Online **PAPER**



Cite this: Soft Matter, 2023, **19**, 4859

Received 16th November 2022, Accepted 24th May 2023

DOI: 10.1039/d2sm01508k

rsc.li/soft-matter-journal

The alternate ligand Jagged enhances the robustness of Notch signaling patterns†

Mrinmov Mukheriee ** and Herbert Levine**

The Notch pathway, an example of juxtacrine signaling, is an evolutionary conserved cell-cell communication mechanism. It governs emergent spatiotemporal patterning in tissues during development, wound healing and tumorigenesis. Communication occurs when Notch receptors of one cell bind to either of its ligands, Delta/Jagged of the neighboring cell. In general, Delta-mediated signaling drives neighboring cells to have an opposite fate (lateral inhibition) whereas Jagged-mediated signaling drives cells to maintain similar fates (lateral induction). Here, by deriving and solving a reduced set of 12 coupled ordinary differential equations for the Notch-Delta-Jagged system on a hexagonal grid of cells, we determine the allowed states across different parameter sets. We also show that Jagged (at low dose) acts synergistically with Delta to enable more robust pattern formation by making the neighboring cell states more distinct from each other, despite its lateral induction property. Our findings extend our understanding of the possible synergistic role of Jagged with Delta which had been previously proposed through experiments and models in the context of chick inner ear development. Finally, we show how Jagged can help to expand the bistable (both uniform and hexagon phases are stable) region, where a local perturbation can spread over time in an ordered manner to create a biologically relevant, perfectly ordered lateral inhibition pattern.

1. Introduction

Notch signaling plays a crucial role in controlling cell-fate decisions during embryonic development.^{1,2} The signaling cascade is initiated via ligand binding to Notch transmembrane receptors, leading to the release of the Notch Intercellular Domain (NICD) and downstream regulation by NICD of its target genes. 1,3-5 This simple mechanism regulates cell-fate differentiation in different biological systems ranging from the development of the inner ear,6,7 vascular smooth muscle cell development,⁵ Drosophila wing disk formation,¹ bristle patterning⁵ and cancer metastasis.⁸⁻¹¹

There are two types of ligands, Delta-like and Jagged-like, which can bind to the Notch receptors on the surface of a neighboring cell, as examples of juxtacrine signaling. The signal can introduce biochemical feedback between neighboring cells coordinating their cell-fate, which leads to spatiotemporal pattering in multicellular systems. Notch-ligand binding can also happen in the same cell (cis-coupling) apart from the usual interaction between neighboring cells (trans-coupling). 12,13

In general, Delta-mediated Notch signaling drives neighboring cells to have an opposite fate, which creates an alternating 'salt and pepper' pattern of Sender (high ligand, low receptor) and Receiver (low ligand, high receptor) cells in tissue; this is referred to as lateral inhibition. Alternatively, Jagged almost always promotes a similar cell-fate in neighboring cells, giving rise to lateral induction; see ref. 14 for a rare counter-example. The full Notch-Delta-Jagged system can act as a three-way switch, giving rise to an additional hybrid state (medium ligand, medium receptor). 15,16 Also, at an intermediate baseline production rate, adding Jagged to the pure Notch-Delta system has been suggested as a mechanism to alter the accuracy 17 and robustness⁷ of the patterns in various developmental processes. In fact, the possible cooperation of Jagged with Delta in forming robust lateral patterns has been presented through experiment and theoretical models for the first time in the context of chick inner ear development⁷ and later generalized by additional computational modeling.¹⁸

In this paper, we study the pattern formation problem in the Notch-Delta-Jagged system, extending the framework¹⁹ previously used for the Notch-Delta system by including the Jagged ligand. Inspired by the general tissue structure in epithelial monolayers which roughly form a hexagonal lattice,8 we evaluate the dynamics of Notch, Delta, Jagged and NICD on a 2d hexagonal array of cells. We calculate the regions of phase space across different parameters for which stable (ordered)

^a Center for Theoretical Biological Physics, Northeastern University, Boston, MA, USA. E-mail: mr.mukherjee@northeastern.edu

^b Depts. of Physics and Bioengineering, Northeastern University, Boston, MA, USA

[†] Electronic supplementary information (ESI) available. See DOI: https://doi.org/

solutions exist. We mainly focus on the dose-dependent role of Jagged and how it can affect the accuracy and robustness of disordered patterns, generated from uniform (with small noise) initial conditions. In the end, we discuss how an expanded region of bistability (where both uniform and hexagon stable phases coexist) can arise in the presence of Notch-Jagged signaling and help to form perfectly ordered patterns. This can be a useful strategy to obtain accurate patterns in noisy biological systems.

Our work is motivated by a number of experimental facts seen in Notch systems. One of the interesting observations regulating Notch system patterning is the lack of anti-hexagon patterns. In most cases studied to date, the high Delta cells, which are typically the most differentiated cell type, lie at the center of the roughly hexagonal patterns surrounded by high Notch cells. This feature is one aspect of the system that should be explained by a computational model, and we will see that Jagged tends to suppress the antihexagon (high Notch surrounded by high Delta) alternative. A second motivation is the need to understand the relative robustness of the spatial ordering, even in the presence of inevitable fluctuations in cell shape and geometry. This issue has led to suggestions of a number of possible auxiliary mechanisms. Results here will show that the inclusion of Jagged signaling does not completely solve this robustness problem but does help significantly in this regard. This finding is in line with less rigorous arguments to this effect presented in ref. 10. Our results augment results in ref. 18 in showing new aspects of Delta-Jagged synergy and in extending the range of modeling assumptions under which it can occur.

2. Model

Here, we study the Notch-Delta-Jagged system on a 2d hexagonal array of cells. To incorporate both the basic features of Notch-Delta signaling induced lateral inhibition pattern (Fig. 1a) and Notch-Jagged signaling induced lateral induction pattern (Fig. 1b), we use the following deterministic ordinary differential equations (ODEs)15,16 based on previously introduced models, $^{13,20-22}$ involving the concentrations of Notch (N), Delta (D), Jagged (I) and NICD (I),

$$\dot{N}_{x} = \lambda_{N} H_{+}(I_{x}) - k_{c} N_{x} (D_{x} + J_{x}) - k_{t} N_{x} (D_{x}^{\text{ext}} + J_{x}^{\text{ext}}) - \gamma N_{x}$$

$$\dot{D}_{x} = \lambda_{D} H_{-}(I_{x}) - k_{c} D_{x} N_{x} - k_{t} D_{x} N_{x}^{\text{ext}} - \gamma D_{x}$$

$$\dot{J}_{x} = \lambda_{J} H_{+}(I_{x}) - k_{c} J_{x} N_{x} - k_{t} J_{x} N_{x}^{\text{ext}} - \gamma J_{x}$$

$$\dot{I}_{x} = k_{t} N_{x} (D_{x}^{\text{ext}} + J_{x}^{\text{ext}}) - \gamma_{I} I_{x}$$
(1)

where, x refers to the positions of the cells on the hexagonal lattice. $H_+(I)=1+rac{I^n}{1+I^n}$ and $H_-(I)=rac{1}{1+I^n}$ are the Hill functions to represent the effect of NICD (I) (via transcriptional regulation) on the production rate of Notch (N), Delta (D) and Jagged (J). k_c and k_t are the strengths of cis-inhibition

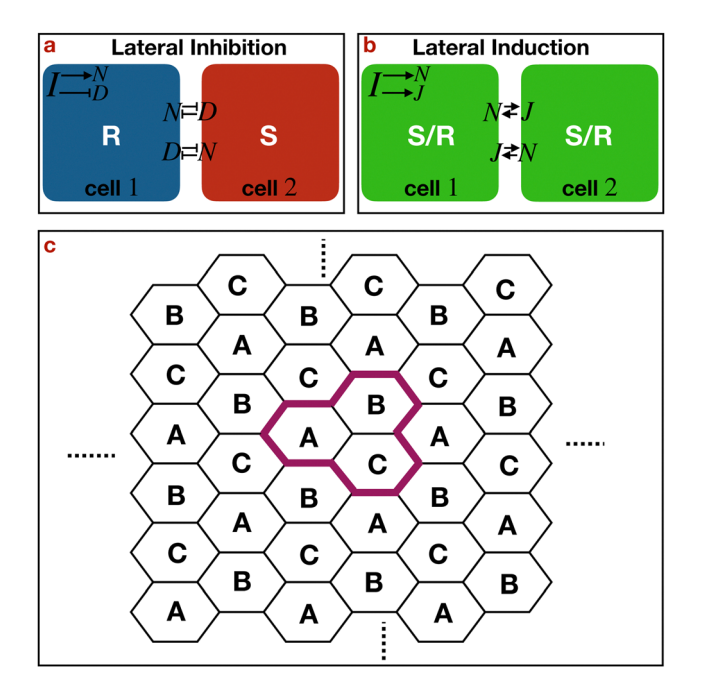


Fig. 1 Schematics of lateral inhibition and lateral induction. Schematic diagram of (a) lateral inhibition between two neighboring cells, (b) lateral induction between two neighboring cells and (c) a hexagonal lattice system spanned by A-B-C unit cells.

and trans-activation respectively. λ_N , λ_D and λ_I are the baseline production rates of N, D and J respectively. γ represents the degradation rate of N, D, I (assumed equal) and γ_I the degradation rate of I. $(N, D, J)^{\text{ext}}$ refers to the average over the 6 nearest neighbors of cell x.

We use a baseline set of parameters taken from the literature: ${}^{15,16,19}k_c = 0.1, k_t = 0.04, \gamma = 0.1, \gamma_I = 0.5$, the Hill coefficients for Notch and Delta $(n_N = n_D = 2)$ and for Jagged $(n_J = 5)$ and vary λ_N , λ_D and λ_I . These parameters were not derived by fitting our model to some specific experimental system and dataset. Instead, we chose typical physiological values based on a number of studies and experimental realizations and investigated the generic features of the resultant dynamical system. We also investigated the effect of varying individual parameters (for example, k_c and k_t) to investigate the specific roles played by different interactions. For a fuller description of this approach, see ref. 19 and the Results and discussion section of this work. All the parameters used in the figures throughout the manuscript are listed in Table S1 (see the ESI†).

We are interested in hexagonal ordered patterns. These patterns on a hexagonal lattice are invariant under the translation with vectors $\pm 6\hat{x}$, $\pm 3\hat{x} \pm 3\sqrt{3}\hat{y}$ (\hat{x} , \hat{y} , are the unit vectors along the axes (xy) and the unit length is 1/2 the length of the hexagonal sides). Thus, the concentrations of Notch (N), Delta (D), Jagged (J) and NICD (I) everywhere on the lattice are completely determined by their concentrations on the cells labelled by A, B and C (Fig. 1c). Thereby, the entire problem (eqn (1)) of hexagonal ordered patterns for a multicellular system is reduced to 12 coupled ODEs (explicit equations given in the ESI†). The details of the methods to generate all the

figures in this article are given in the ESI.† The codes are available at https://github.com/mrinmoy169/Notch Delta Jagged.

3. Results and discussion

3.1. Phase diagrams

We solve the reduced set of ODEs numerically to find the parts of parameter space for which the uniform state $((N, D, J, I)_A = (N, D, I$ $(J, I)_B = (N, D, J, I)_C$ is unstable with respect to perturbations. First, we find the fixed points where $\dot{N} = \dot{D} = \dot{I} = 0$ and analyze their stability via linear stability analysis (for details see the ESI†) across the parameter space. For a fixed value of λ_N and λ_I the uniform solution becomes unstable for $\lambda_D > \lambda_D^{U}(\lambda_N, \lambda_I)$ via a transcritical bifurcation (Fig. 2) and overlaps non-uniform solutions where the concentrations on two sublattices (say B, C) are always identical, differing from the concentrations on the remaining sublattice A, such that, $(N,D,J,I)_B = (N,D,J,I)_C \neq (N,D,J,I)_A$. There are two types of these hexagonal solutions; \'hexagon' (high D cells surrounded by high N cells), and 'antihexagon' (high N cells surrounded by high D cells). Labeling the high D cells as 'Senders' (S) and low D cells as 'Receivers' (R), the hexagon (H) and anti-hexagon (A) solutions are defined as $(\Delta N < 0, \Delta D > 0)$ and $(\Delta N > 0, \Delta D < 0)$ respectively, where ΔN and ΔD are defined as $(N_S - N_R)$ and $(D_{\rm S}-D_{\rm R})$ respectively.

In Fig. 2, we show a bifurcation diagram description of the onset of pattern formation as the Delta production is varied. For all these curves, $\lambda_D \gg \lambda_J$, *i.e.* Delta is the dominant Notch ligand. Different sub-figures refer to different Notch production rates. In general, the uniform state loses stability via a transcritical bifurcation. Notice however the proximity between the transcritical bifurcation point and a nearby saddle-node altering the stability of one or both of the hexagonal branches (Fig. 2a and b). This suggests that the system possesses a codimension 2 pitchfork bifurcation reflecting the coalescence of the transcritical and saddle-point bifurcations. Indeed, for a fixed value of λ_I , there is always a fixed value of $\lambda_N = \lambda_N^{PF}(\lambda_I)$

where the pitchfork bifurcation occurs; this point is seen in Fig. 2c. At $\lambda_N = \lambda_N^{\rm PF}(\lambda_I)$, the stable uniform (U) state becomes unstable (with 2 unstable modes) at $\lambda_D > \lambda_D^{\text{U}}(\lambda_N, \lambda_I)$ and two new states are born, a stable H and an unstable A. The interesting point is that this point appears to occur in a physically possible and experimentally plausible 13 range of parameters. For all other values of λ_N , the pitchfork breaks up into separate transcritical and saddle-node bifurcations, as already discussed. For detailed discussion of this diagram for the case of a pure Notch-Delta system see ref. 19.

Given the above, we can determine the stable states as a function of the two parameters, λ_N and λ_D . The overall diagrams are presented in Fig. 3a-e for different values of λ_I . The representative hexagon and antihexagon patterns are shown in the inset of Fig. 3c. For $\lambda_N > \lambda_N^{PF}(\lambda_I)$ and $\lambda_D > \lambda_D^{U}(\lambda_N, \lambda_I)$, the only solutions that survive are stable hexagon (H), which is in accord with the general biological finding of the absence of antihexagon phases in nature. Also, λ_N^{PF} decreases with the increase in λ_{I} , which broadens the possibility of getting hexagon phases at smaller values of λ_N . On the other hand, for $\lambda_N < \lambda_N^{\rm PF}(\lambda_I)$ especially at higher values of λ_I , there is only a small region of parameter space for which the antihexagon (A) phases are stable; this helps ensure the low likelihood of antihexagon (A) phases in a biological environment with insufficient parameter control.

Importantly, the range of parameter space where the stable uniform and stable hexagon phases coexist widens significantly as λ_I increases (Fig. 3f). Later, we will discuss the implication of this bistable region for the issue of how it might be possible to create perfectly ordered patterns.

In general, for stable patterns the N and D values are anticorrelated in a cell, whereas N and I are correlated; furthermore, the cells with high D (labeled as Sender, S) will have low N and I (Fig. S2 in the ESI†). These specific correlations ensure the fate of a cell in development, e.g., in the case where of the developed inner ear hair cells (Senders) express high D and the surrounding supporting cells (Receivers) express high

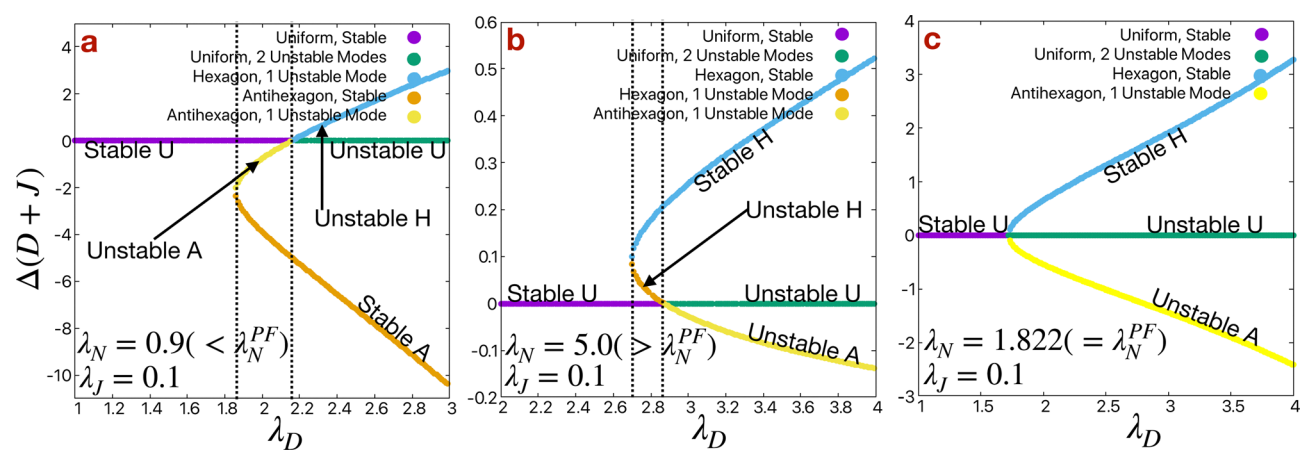


Fig. 2 Bifurcation diagram. Bifurcation diagrams for (a) $\lambda_N < \lambda_N^{\rm PF}$, (b) $\lambda_N > \lambda_N^{\rm PF}$ and (c) $\lambda_N = \lambda_N^{\rm PF}$ at $\lambda_J = 0.1$. All other parameters are standard. $\Delta(D + J)$ is defined as $(D_S + J_S - D_R - J_R)$, where S and R represent the Sender (high D, low N) and Receiver (low D, high N) states respectively. There is no practical difference between D + J versus D in our parameter range, so we have just referred to the D pattern in the text.

Paper Soft Matter

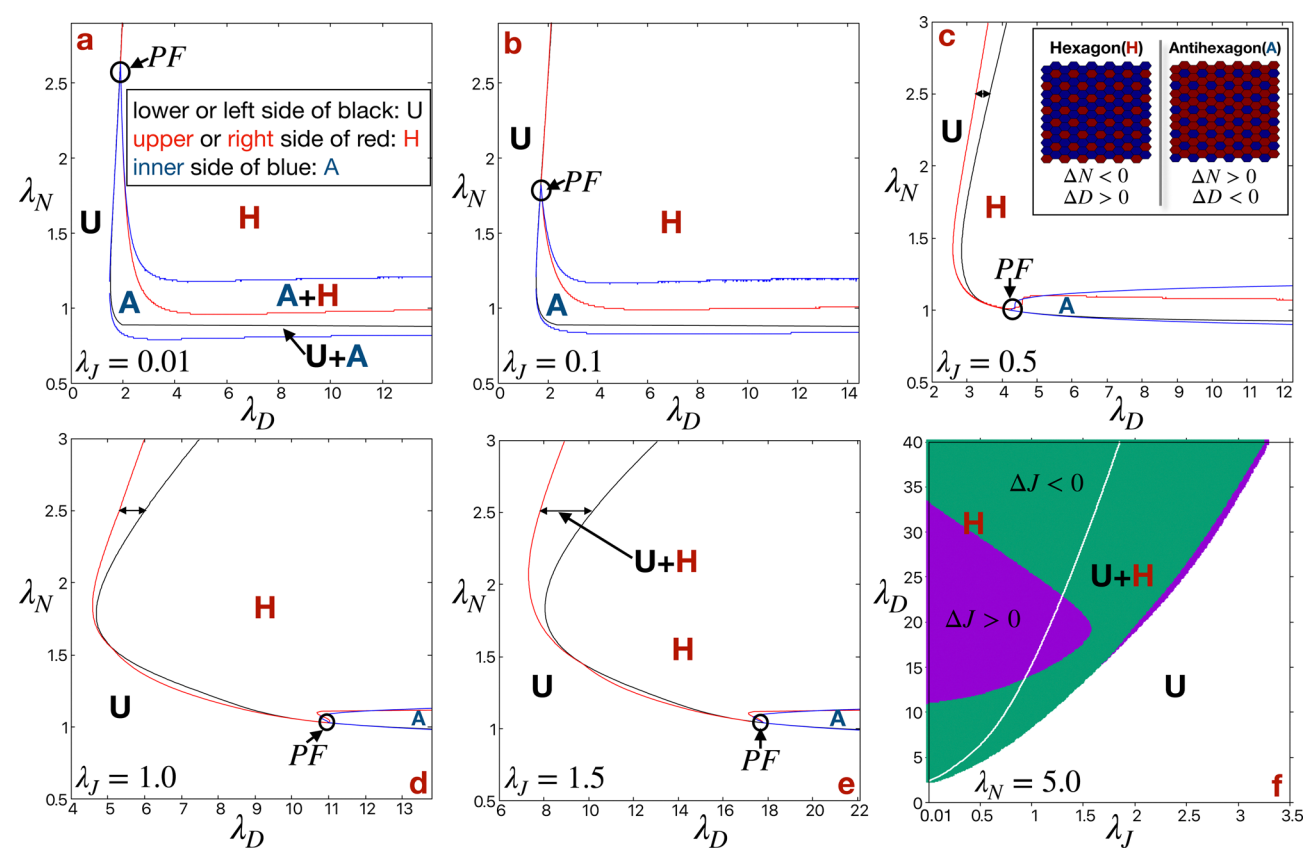


Fig. 3 Phase diagrams. Phase diagrams in the $\lambda_N - \lambda_D$ plane consist of the regions of stable uniform (U: $\Delta N = \Delta D = 0$), hexagon (H: $\Delta N < 0$, $\Delta D > 0$), antihexagon (A: $\Delta N > 0$, $\Delta D < 0$) phases and different bistable regions (U + A, U + H, A + H) for (a) $\lambda_J = 0.01$, (b) $\lambda_J = 0.1$, (c) $\lambda_J = 0.5$, (d) $\lambda_J = 1.0$ and (e) $\lambda_J = 1.5$. In each phase diagram, the lower or left side of black lines represents the region of stable uniform (U) phases, the upper or right side of the red lines represent the region of stable hexagon (H) phases, the inner side of blue lines represent the region of stable antihexagon (A) phases and the point indicated by the small black circles, where U, A and H meet represent the point of pitchfork bifurcation. The inset in (c) represents the hexagon (H) and antihexagon (A) patterns of Delta (D) on a hexagonal lattice. (f) Phase diagram in the $\lambda_D - \lambda_J$ plane for $\lambda_N = 5.0$. The white and colored (green: $J_S < J_R$ $(\Delta J < 0)$ and purple: $J_S > J_R (\Delta J > 0)$ regions represent uniform (U) and hexagon (H) phases respectively. The white line represents the boundary of the U region. ΔN , ΔD and ΔJ are defined as $(N_S - N_R)$, $(D_S - D_R)$ and $(J_S - J_R)$ respectively, where S and R represent the Sender (high D, low N) and Receiver (low D, high N) states respectively. All other parameters are standard.

N. But J can be correlated or anti-correlated with D depending on the specific point of the parameter space (in the purple region of Fig. 3f D and I are correlated, whereas in the green region they are anti-correlated). Then the immediate question arises: does this non-specific correlation between D and I affect the specification of cells' fate? The answer appears to be no; the very much smaller difference in I between the Sender (S) and Receiver (R) cells with respect to the similar difference in D $(\Delta J/\Delta D \sim 10^{-2})$ across our entire parameter range, ensures the lesser importance of J with respect to D for the specification of a cells' fate.

3.2. Disorder in the pattern formation

In the previous section, we found regions of parameter space in which hexagon phases are stable and ordered. Considering the perfectly ordered states as a final pattern allowed us to simplify the problem to a reduced set (12) of ODEs instead of solving $4L^2$ ODEs on a hexagonal lattice of size L (total number of cells L^2). We note that our numerical studies revealed no evidence of linear instabilities that do not

respect the reduced system symmetry; all the unstable modes responsible for the results of Fig. 2 are "local" instabilities of the 12 ODE system.

The question then arises as to how these patterns can be generated in the case of a realistic noisy biological environment. We focus here on stochasticity in the initial configuration at the moment when the system is switched into a parameter range allowing pattern formation. Starting from a uniform solution (no pattern) with small fluctuations (noise) on a hexagonal lattice of size L in the parameter space ($\lambda_N = 5.0$, $\lambda_D = 10.0$, $\lambda_I = 0.5$, all other parameters are standard), where the uniform state is linearly unstable, the final stable patterns are ordered for L = 6 (Fig. 4a) and disordered for L = 50 (Fig. 4b). The patterns of all the fields N, D, J and I are shown in Fig. S1 in the ESI.† For large system size L = 50, the patterns are disordered with many domain boundaries formed between the hexagon patterns which nucleate and spread on different sublattices. The time evolution of D for all the cells is shown in Fig. 4c and Video S1 (ESI \dagger) (for L = 6) and Video S2 (ESI \dagger) (for L = 50).

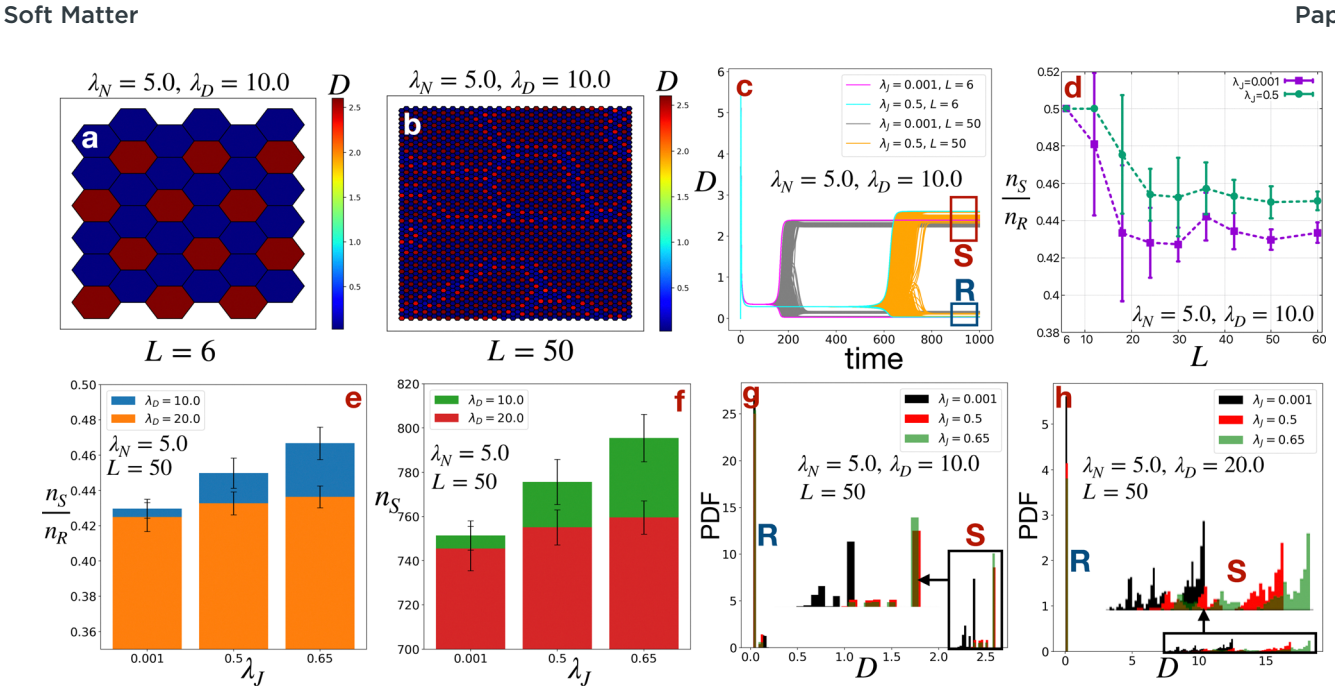


Fig. 4 Disorders in patterns. Steady state patterns of Delta (D) at $\lambda_N = 5.0$, $\lambda_D = 10.0$, and $\lambda_J = 0.5$ for two different system sizes (a) L = 6 (ordered) and (b) L=50 (disordered). (c) Dynamics of Delta (D) for all the cells in a hexagonal lattice of size L=6 and L=50 at $\lambda_N=5.0$, $\lambda_D=10.0$, $\lambda_J=0.001$ and 0.5. The branches enclosed in the red and blue rectangles represent the Sender (S: high D) and Receiver (R: low D) cells respectively. (d) The ratio of the number of Sender (S) and Receiver (R) cells in steady states $\left(\frac{n_{\rm S}}{n_{\rm R}}\right)$ as a function of system size L at $\lambda_N=5.0$, $\lambda_D=10.0$, and $\lambda_J=0.001$ and 0.5. (e) The same ratio $\left(\frac{n_{\rm S}}{n_{\rm R}}\right)$ and (f) number of Sender (S) states (n_S) for L=50 at $\lambda_J=0.001$, 0.5 and 0.65 for different values of λ_D at $\lambda_N=5.0$. Probability density (PDF) of Delta (D) in the steady states for system size L=50 at (g) $\lambda_N=5.0$, $\lambda_D=10.0$ and (h) $\lambda_N=5.0$, $\lambda_D=20.0$. The insets in (g and h) show the enlarged version of the PDF of the Sender (S) states. All other parameters are standard

The ratio between high D(S) and low D(R) cells $\left(\frac{n_S}{n_R}\right)$ roughly estimates the degree of disorder in steady state patterns. For a perfectly ordered pattern this ratio should be close to 0.5 (for L = 50, $n_{\rm S} = 825$ and $n_{\rm R} = 1675$). $\frac{n_{\rm S}}{n_{\rm R}}$ decreases gradually as Lincreases and starts to saturate for L > 18 (Fig. 4d). For a larger system the nucleation centers for hexagonal patterns are more plentiful, which leads to higher disorder in the patterns. But, $\frac{n_{\rm S}}{n_{\rm R}}$ increases with the increase in λ_I across different L (Fig. 4d) and λ_D (Fig. 4e). The time evolution and steady state patterns of D for different values of λ_D are shown in Fig. S2 in the ESI.† The increase in $\frac{n_{\rm S}}{n_{\rm R}}$ or $n_{\rm S}$ (Fig. 4e) with an increase in λ_J and/or decrease in λ_D indicates that we can find the maximum number of Sender cells near the stability boundary of the uniform (U) phase (the white line in the phase diagram in Fig. 3f). Similarly, the phase diagrams in Fig. 3a–e also suggest that the n_S should increase as λ_N decreases. We do observe a gradual increment in $n_{\rm S}$ or $\frac{n_{\rm S}}{n_{\rm P}}$ as λ_N decreases (Fig. S3a and c in the ESI†). For very small values of $\lambda_N = 1.5$, we find a different kind of disordered pattern where two neighboring cells can have high D (Fig. S3a and Video S3, ESI†), which leads to $n_{\rm S} > 825$ or $\frac{n_{\rm S}}{n_{\rm R}} > 0.5$. This situation can also be remediated by increasing λ_J . That is, higher λ_I , at this smaller value of $\lambda_N = 1.5$, decreases the possibility of getting two neighboring high D cells and

hence leads towards more ordered patterns (Fig. S3b and d in the ESI†).

We also observed a wide distribution of D values among the high D, Sender (S) cells (Fig. 4g and h). The long tail in the distributions arises from the cells at the hexagonal domain boundaries of the disordered patterns. Conversely, most of the cells at the core of the hexagonal domains express similar values of D to the values of D for perfectly ordered patterns, as we found for L = 6 (Fig. 4c). In general, we need additional strategies, beyond shifting the system such that parameters lie closer to the boundary of stable uniform solutions, in order to get perfectly ordered patterns in a biological system; we will return to this below. But, an increment in the number of high D cells with an increase in λ_I near the boundary of the stable uniform regions of the phase spaces, may have other implications in biological systems. For example, in case of collective migration a larger number of high D cells can increase the overall invasiveness; highly invasive or leader cells express high D. 23,24

Moreover, the time to reach the steady state (differentiation time) increases as λ_I increases (Fig. 4c). This is again because higher λ_I shifts the system towards stability of the uniform state, which then increases the differentiation time. This slow differentiation time can accommodate other slow processes of error correction in the pattern formation such as a large delay in protein production.²⁵ The increase in patterning time that occurs with increasing Jagged production can serve to

distinguish this parameter variation versus changes in cisinhibition (to be discussed below) that actually speed up the process.

3.3. Dose-dependent role of Jagged

Depending on the baseline production rate of Jagged (λ_I) the cells can attain different fates. Starting from a lateral inhibition pattern of high D (low I, low N) Sender (S) and low D (high I, high N) Receiver (R) cells at small values of λ_I , a hybrid (S/R) state with intermediate values of $I^{15,16}$ appears as λ_J increases (Fig. 5a). Note that at low λ_I , where the Notch-Delta signaling dominates, Jagged acts synergistically with Delta to refine the lateral inhibition pattern of Sender and Receiver cells. The addition of Jagged to Delta in binding the common resource of Notch receptors leads to the greater activation of NICD and hence stronger suppression of Delta in the neighboring Receiver cells. We quantify this by calculating the difference in Delta (ΔD) between the Sender and Receiver cells ($D_{\rm S}-D_{\rm R}$) as a function of λ_I , considering the perfectly ordered patterns where at steady state all the Sender and Receiver cells attain specific $D_{\rm S}$ and $D_{\rm R}$ values respectively. We observe a non-monotonic dependence of ΔD as a function of λ_I across different values of λ_D (Fig. 5b). Up to a certain value of λ_J , ΔD increases gradually and reaches a maximum; with the further increase in λ_I the strength of Notch-Delta and Notch-Jagged signaling becomes comparable, the system enters into a region of bistability where both the uniform (U) and hexagon (H) phase are stable, and eventually ΔD starts to decrease gradually. Both $D_{\rm R}$ and $D_{\rm S}$ increases as λ_I increases up to the critical value of λ_I (Fig. S4 in the ESI \dagger), but the increment in D_S is always much higher than the increment in D_R . At a fixed value of λ_L , the competition between D and J, and thus the value of ΔD can be enhanced by either increasing λ_D at fixed λ_N (Fig. 5b) or decreasing λ_N at fixed λ_D (Fig. S4d and e in the ESI†). At very high values of λ_I , lateral

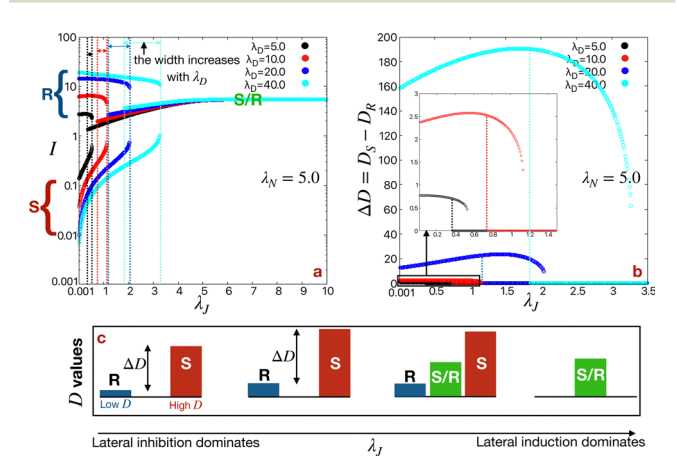


Fig. 5 Dose-dependent role of Jagged (J). (a) NICD (I) as a function of λ_J showing the Sender (S: high D), Receiver (R: low D) and hybrid S/R (intermediate D) state branches. (b) The difference in Delta (ΔD) between the S and R cells ($D_S - D_R$) as a function of λ_J . The inset shows an enlarged version of the rectangular region at very small values of ΔD . All other parameters are standard. (c) Schematic representation of R, S and S/R states and their Delta (D) values as a function of λ_J .

induction dominates and the pattern becomes uniform consisting entirely of hybrid S/R cells. Hybrid S/R states have a critical role in promoting collective migration in wound healing²⁶ and cancer metastasis. 16 This dose-dependent role of Jagged is shown in the schematic diagram in Fig. 5c.

This synergistic role of Jagged with Delta enabling the robust lateral inhibition pattern of high D hair cells surrounded by low D supporting cells has been suggested experimentally in the hair cell differentiation phase of chick inner ear development. It is worth noting, however, that in the context of inner ear development, cis-inhibition does not appear to be very important; this means that results based on our baseline parameter set reflecting significant cis-inhibition may not be directly applicable to this particular system. We will discuss the effects of varying cis-inhibition on the competition between Jagged and Delta in the next section. This idea of synergy has also been proposed in a model of angiogenesis so as to enable the robust patterning of high D, Tip and low D, Stalk cells.^{27,28}

3.4. Effect of cis-inhibition and trans-activation strength

Although *cis*-inhibition (k_c) does not directly contribute to the production of the NICD signal, it affects the patterns by altering the Notch, Delta and Jagged expressions. It has been shown that k_c increases the robustness of lateral inhibition patterns by inactivating Notch in Sender cells. At first, we draw a phase diagram in the λ_D - k_c plane for a smaller value of $\lambda_I = 0.1$ (Fig. S5a in the ESI†). We find a new kind of surprising stable state with N and D correlated for very small values of k_c (cvan and orange colored region in the phase diagram in Fig. S6a, ESI \dagger). As opposed to the usual anti-correlation of N and D values in a cell, here both $\Delta N > 0$ and $\Delta D > 0$. We refer to these solutions as High-High (Hi-Hi), since both the D and Nare higher in Sender cells compared to those in Receiver cells. As discussed in ref. 19, these kinds of states have not been observed experimentally to date, presumably because the parameters for which these solutions exist are not typically found in any developmental process. Apart from that, at higher λ_I these Hi-Hi states do not exist even at smaller values of k_c as the patterns become uniform (Fig. 6a).

As k_c increases, we move further away from the boundary of the stable uniform phases (white line in the phase diagram in Fig. 6a), which decrease the number of Sender cells (n_S) by creating more disordered states (Fig. 6b). This can be again remediated by increasing λ_I as shown in Fig. 6b. Also as k_c increases, a higher value of λ_I is needed to obtain stable hexagon patterns (Fig. 6a). The higher values of λ_I allow higher values of ΔD (at fixed k_c), and hence increases the robustness of the patterning. In general, ΔD increases with an increase in k_c up to a certain value of k_c and then starts to saturate (Fig. 6c). Surprisingly, ΔD decreases as k_c increases for very small values of $\lambda_I = 10^{-3}$. Actually, this behavior depends on the relative availability of Notch and Delta. Thus, the dependence of ΔD on k_c can be switched by either increasing λ_D at fixed λ_N (Fig. S5b in the ESI†) or decreasing λ_N at fixed λ_D (Fig. S5c in the ESI†).

As opposed to k_c , the *trans*-activation strength (k_t) interacts with λ_I in an opposite manner. Smaller values of k_t broaden the

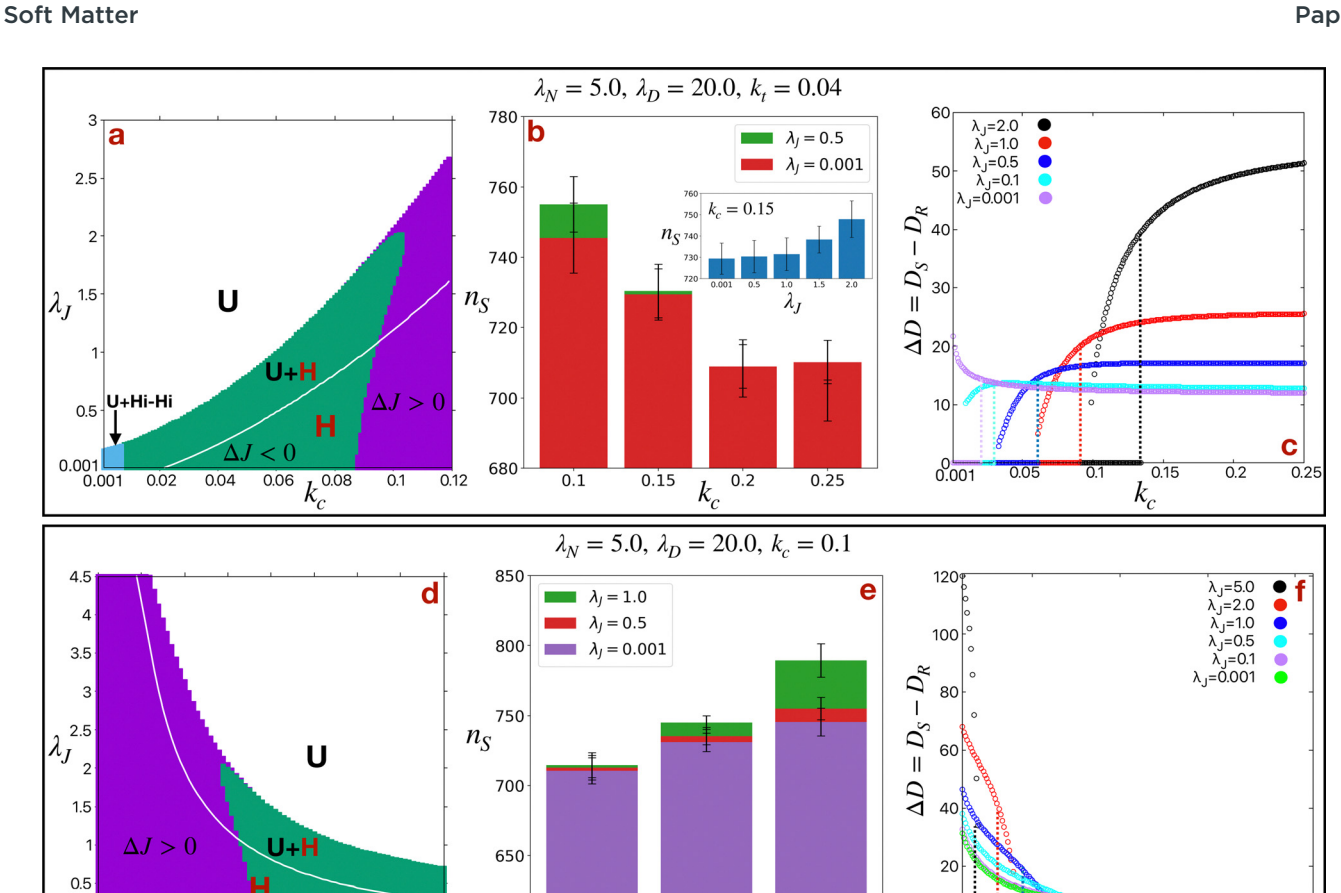


Fig. 6 Role of cis-inhibition (k_c) and trans-activation (k_t). (a) Phase diagrams in the $\lambda_J - k_c$ plane for $\lambda_N = 5.0$, $\lambda_D = 20.0$ and $k_t = 0.04$. The white and colored (green: $\Delta J < 0$) and purple: ($\Delta J > 0$)) regions represent uniform (U: $\Delta N = \Delta D = 0$) and hexagon (H: $\Delta N < 0$, $\Delta D > 0$) phases respectively. The cyan colored region represents the bistability of uniform (U) and High-High (Hi-Hi: $\Delta N > 0$, $\Delta D > 0$) phases. The white line represents the boundary of the U region. ΔN , ΔD and ΔJ are defined as $(N_S - N_R)$, $(D_S - D_R)$ and $(J_S - J_R)$ respectively, where S and R represent the Sender (high D, low N) and Receiver (low D, high N) states respectively. (b) The number of Sender (S) states (n_S) and (c) the difference in Delta (ΔD) between the Sender (S) and Receiver (R) states ($D_S - D_R$) as a function of k_C for different values of λ_J at $\lambda_N = 5.0$, $\lambda_D = 20.0$, $k_t = 0.04$ for a hexagonal lattice of size L = 50. The inset in (b) shows the number of Sender (S) cells (n_S) as a function of λ_J at a fixed value of $k_C = 0.15$. The similar (d) phase diagram in the $\lambda_J - k_t$ plane, (e) number of Sender (S) cells (n_S) as a function of k_t and (f) difference in Delta (ΔD) between the Sender (S) and Receiver (R) cells $(D_S - D_R)$ as a function of k_t for $\lambda_N = 5.0$, λ_D = 20.0, and k_c = 0.1. All other parameters are standard.

0.03

0.04

0.02

range of λ_I for which hexagon phases are stable (Fig. 6d). Furthermore, n_S increases and ΔD decreases as k_t increases. In short, in the presence of higher λ_L , higher values of k_c and/or lower values of k_t increase the robustness (higher values of ΔD) of the patterns.

0.06 0.07

3.5. Ordered patterns, revisited

As discussed earlier, the pattern arising from the uniform states with small noise are in general disordered, with many domains of hexagon patterns. The hexagon patterns randomly nucleate at different sublattices and spread over time in a disordered manner. One way to avoid this disorder can be to find a parameter set for which a local perturbation which nucleates the pattern would spread over time in a ordered manner to create a perfectly ordered pattern.²⁹ This can happen in the bistable region, where both the uniform and hexagon phases are stable (Fig. 3).

Fig. 7 shows the spatiotemporal patterns of D on a hexagonal lattice starting from a hexagonal seed in the center of the lattice, for different parameters. For the parameter space $(\lambda_N = 5.0, \lambda_D = 10.0, \lambda_I = 0.5, \text{ all other parameters are standard})$ where only the hexagon phase is stable, and as expected the pattern nucleates at different sublattices and spreads over time in a disordered manner (Fig. 7a and Video S4, ESI†). But, for the parameter set ($\lambda_N = 5.0$, $\lambda_D = 10.0$, $\lambda_I = 0.9$, all other parameters are standard) chosen from the region of bistability, the initial hexagonal seed spreads over time in a ordered manner and thereby creates a perfectly ordered pattern (Fig. 7b and Video S5, ESI†).

In the generic Notch-Delta system without Jagged, the parameter range exhibiting this bistability is very narrow (Fig. 3c). But, including finite λ_I widens the range significantly (Fig. 3f). We can also investigate the effect of different parameters on the width of the region of bistability by computing the phase diagrams in the λ_D - λ_I plane (Fig. S6 in the ESI†). We observe that the region of bistability in the phase space increases, especially at higher values of λ_D and λ_I , as λ_N increases and/or **Paper** Soft Matter

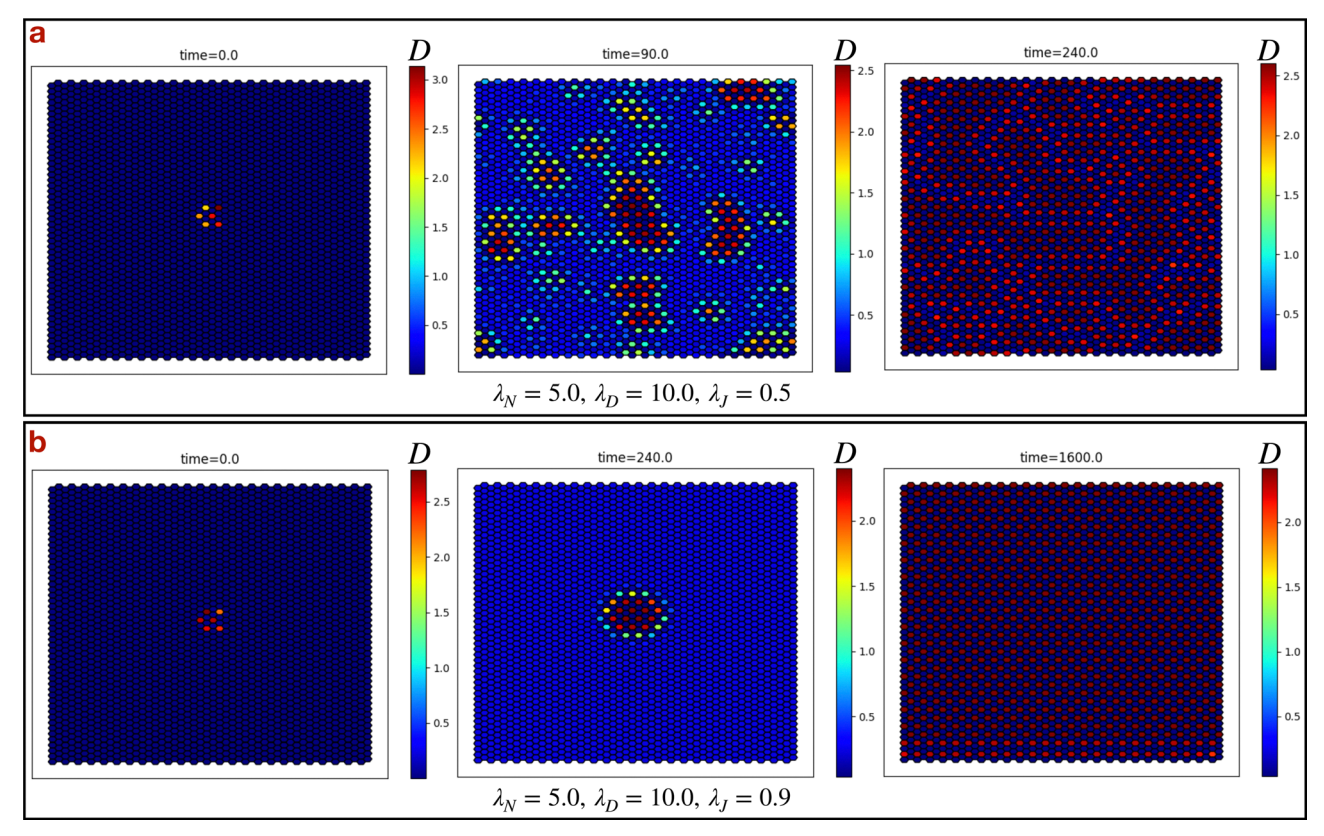


Fig. 7 Spatiotemporal patterns of Delta (D) starting from a hexagonal seed. (a) The steady state patterns are imperfect (disordered) for the parameters $\lambda_N = 5.0$, $\lambda_D = 10.0$ and $\lambda_J = 0.5$, where only the hexagon (H) phase is stable. (b) The steady state patterns are ordered for the parameters $\lambda_N = 5.0$, λ_D = 10.0 and λ_J = 0.9, where both the hexagon (H) and uniform (U) phases are stable (bistable region). All other parameters are standard

Table 1 Effects of different parameters on stable hexagon pattern formation

Parameters	$n_{\rm S}$	Differentiation time	ΔD	Bistable region
$\lambda_N \uparrow$ $\lambda_D \uparrow$ $\lambda_f \uparrow$ $k_c \uparrow$ $k_t \uparrow$	${\longrightarrow}{\longleftarrow}$	↓ ↑ ↓	→ ↑ ↑ ↑	† † †

 k_c decreases and/or k_t increases. Thus, Jagged helps to widen the bistable region, which can help to obtain ordered hexagon patterns in the biological system with weaker control of operating parameters.

4. Conclusions

In this paper, we explored the pattern formation in the Notch-Delta-Jagged signaling on a multicellular system. Assuming hexagonal symmetry of a cellular lattice (as being close to biological tissue) helps us to compute the phase space by reducing the problem of ordered patterns to a set of 12 coupled ODEs. Throughout the paper, we focus on the effect of Jagged on the accuracy and robustness of the pure Notch-Delta pattern. We observe that Jagged decreases the possibility of obtaining nonphysical antihexagon states by shrinking the parameter range for which antihexagon solutions are stable. Higher production of Jagged (λ_I) also ensures the absence of experimentally unseen Hi-Hi states (where both Notch and Delta are high in Sender cells) at small values of the cisinhibition rate (k_c) .

In general, starting from a uniform state with small fluctuations, incommensurate hexagon patterns emerge on different sublattices and the pattern spreads in a disordered manner; the final lateral induction pattern contains many domain boundaries between the hexagon structures. We quantified this disorder by calculating the number of Sender cells (n_s) in the lattice. For an ordered lattice of size L (total number of cells = L^2), n_S should be around L/3. Table 1 summarizes the effect of different parameters on n_s . At a fixed value of the other parameters, n_S decreases with the baseline production rate of Notch (λ_N) and/or baseline production rate of Delta (λ_D) and/or cis-inhibition rate (k_c) increases, but n_S increases as the transactivation rate (k_t) increases. In all cases, n_S increases as the baseline production rate of Jagged (λ_I) increases (except for very small values of λ_N), which leads to a more ordered pattern. As a general rule, n_S is the maximum near the stability boundary of the uniform phase. Similarly, the time to reach the steady state (the differentiation time) is maximum near the boundary of the uniform phase, which can be reached by changing the parameters as shown in Table 1. The slow differentiation may allow for other mechanisms to resolve disorders in the pattern.

We quantified the robustness of a pattern by calculating the difference in Delta (ΔD) between the Sender and Receiver cells $(D_{\rm S}-D_{\rm R})$. ΔD increases as λ_I increases up to the point where Notch-Delta signaling no longer dominates over Notch-Jagged signaling. The competition between Delta and Jagged over binding with Notch increases the Delta in Sender cells compared to the Receiver cells. ΔD also increases as λ_D , k_c increases and λ_N , k_t decreases (Table 1).

As listed in Table 1, at sufficiently higher values of λ_N , λ_D , λ_l , and k_t and smaller values of k_c , a large bistable region consisting of uniform and hexagon phases allows the emergence of ordered patterns. Without Jagged-mediated signaling, this bistable region is very narrow. It would be difficult for a biological system to reliably adjust the parameters to lie within the bistable region in the case of small λ_I . In the pure Notch-Delta system without Jagged, many strategies have been proposed throughout the literature to obtain biologically relevant ordered patterns, by adjusting the time delays, 25,30 the noise^{31,32} in the network, coupling a parameter to an initiation wave, 19 or coupling to different properties of cells with a core Notch-Delta circuit such as apoptosis, 33 cell cycle, 34 adhesion, 35,36 cell mechanics, 37-39 etc. The mechanisms mentioned above, along with the Jagged-mediated broadening of the bistable region, should lead to interesting future studies in the Notch-induced pattern formation problem.

The modeling results presented in this paper could be tested in a variety of future experiments. At the most basic level, we would predict that the inhibition of Jagged should give rise to more disorder in developmental systems patterned by notch signaling. This would be accompanied by specific changes in the levels of Delta exhibited by the "center" cells. Similarly, we predict a dose-dependent response to Jagged upregulation, with large upregulation expected to wipe out the pattern completely; this latter effect has been seen in collective migration²³ but not studied to date in developmental processes.

Future research should consider various extensions of the calculations presented here. In ref. 13, a specific algorithm for creating models with controllable levels of structural disorder was introduced. It would be useful to study the role of Jagged in ameliorating the effects of this disorder; unfortunately, this study would be strictly computational as the analysis method used here would not be directly applicable. As already mentioned, another area for future development is the direct coupling of the Notch network to biophysical determinants of cell motility. This is motivated by data showing that high Delta cells become leaders in the collective invasion of both epithelial and endothelial cell layers.40 In accordance with what we observed at high Jagged, data on Jagged over-expression shows the elimination of leader cells in favor of all cells playing an equal role in the collective migration. Also, the Notch signal has directly been implicated as a controller of the EMT cell-fate transition which creates mesenchymal cells from epithelial ones. 41 Reciprocally, mesenchymal cells lose cell-cell contacts and hence limit juxtacrine signaling. Exactly how this all plays out dynamically is a complex issue, which we will report on in future work.

As already mentioned, it should be noted that our paper is not meant to be a precise model of any specific biological realization of Notch patterning. Each of the experimental systems discussed in the literature has a variety of complications involving multiple Notch receptors, multiple Delta ligands, varying degrees of cis-regulation and transcriptional feedback, and a whole host of other factors which couple to the basic elements considered here. The functional forms and the parameters governing all these various interactions are highly uncertain and hence it would be quite difficult to create a completely quantitative version of our model for any of these systems. Instead, our goal was to investigate a basic and somewhat surprising idea, that limited levels of lateral induction can actually strengthen the lateral inhibition process at the heart of much of Notch signaling utility. This idea was already proposed in ref. 7 and 18 and reviewed in ref. 10. Here, we have shown that this Jagged-Delta synergy does not need to rely on direct competition for limited Notch receptor sites but instead can "piggy-back" on the idea that cis-inhibition can favor patterning and hence added cis-inhibition via Jagged can be helpful for lateral inhibition. We have chosen to demonstrate this new feature in a semi-analytic manner by focusing on ordered patterns, their stability, and the ability to converge to these patterns under generic initial conditions. We have also noted the Jagged-dependent contribution to the differences in Delta values between the high and low sites in the hexagonal pattern. We have chosen to do this using rather generic choices for the form of interactions and the parameters contained therein. Thus, our general findings augment other approaches to the same issue and explain earlier results in terms of bifurcation theory and general pattern formation principles. They do not explain the intricate details of any one specific system.

Author contributions

M. M. and H. L. designed the study. M. M. developed the code, performed simulations and analyzed the data. M. M. and H. L. prepared, reviewed and finalized the manuscript.

Conflicts of interest

There are no conflicts to declare.

Acknowledgements

This work was supported by the National Science Foundation by sponsoring the Center for Theoretical Biological Physics award PHY-2019745 and also by award PHY-1605817.

References

- 1 S. J. Bray, Nat. Rev. Mol. Cell Biol., 2016, 17, 722-790.
- 2 A. Bigas and L. Espinosa, Curr. Opin. Cell Biol., 2018, 55, 1-7.
- 3 M. E. Fortini, Dev. Cell, 2009, 16, 633-647.

Paper

4 E. R. Andersson, R. Sandberg and U. Lendahl, *Development*, 2011, **138**, 3593–3612.

- 5 M. Sjöqvist and E. R. Andersson, Dev. Biol., 2019, 447, 58-70.
- 6 J. Neves, G. Abelló, J. Petrovic and F. Giraldez, *Dev., Growth Differ.*, 2013, 55, 96–112.
- 7 J. Petrovic, P. Formosa-Jordan, J. C. Luna-Escalante, G. Abelló, M. Ibañes, J. Neves and F. Giraldez, *Development*, 2014, 141, 2313–2324.
- 8 H. Zhu, X. Zhou, S. Redfield, J. Lewin and L. Miele, *Cancer Res.*, 2013, 73, 410.
- 9 M. Boareto, M. K. Jolly, A. Goldman, M. Pietilä, S. A. Mani, S. Sengupta, E. Ben-Jacob, H. Levine and J. N. Onuchic, *J. R. Soc., Interface*, 2016, **13**, 20151106.
- 10 F. Bocci, J. N. Onuchic and M. K. Jolly, Front. Physiol., 2020, 11, 929.
- 11 J. O. Misiorek, A. Przybyszewska-Podstawka, J. Kałafut, B. Paziewska, K. Rolle, A. Rivero-Müller and M. Nees, *Cells*, 2021, 10, 94.
- 12 A. C. Miller, E. L. Lyons and T. G. Herman, Curr. Biol., 2009, 19, 1378–1383.
- 13 D. Sprinzak, A. Lakhanpal, L. LeBon, L. A. Santat, M. E. Fontes, G. A. Anderson, J. Garcia-Ojalvo and M. B. Elowitz, *Nature*, 2010, 465, 86–90.
- 14 H. Sánchez-Iranzo, A. Halavatyi and A. Diz-Muñoz, *eLife*, 2022, **11**, e75429.
- 15 M. Boareto, M. K. Jolly, M. Lu, J. N. Onuchic, C. Clementi and E. Ben-Jacob, *Proc. Natl. Acad. Sci. U. S. A.*, 2015, 112, E402–E409.
- 16 M. K. Jolly, M. Boareto, M. Lu, J. N. Onuchic, C. Clementi and E. Ben-Jacob, *New J. Phys.*, 2015, 17, 055021.
- 17 B. L. Sheldon and M. K. Milton, Genetics, 1972, 71, 567-595.
- 18 J. C. Luna-Escalante, P. Formosa-Jordan and M. Ibañes, *Development*, 2018, **145**, dev154807.
- 19 E. Teomy, D. A. Kessler and H. Levine, *Phys. Biol.*, 2021, 18, 066006.
- 20 J. R. Collier, N. A. Monk, P. K. Maini and J. H. Lewis, J. Theor. Biol., 1996, 183, 429-446.
- 21 U. Binshtok and D. Sprinzak, *Adv. Exp. Med. Biol.*, 2018, **1066**, 79–98.
- 22 O. Shaya and D. Sprinzak, Curr. Opin. Genet. Dev., 2011, 21, 732-739.
- 23 M. Long, D. D. Zhang and P. K. Wong, *Nat. Commun.*, 2015, 6, 6556.

- 24 P. Torab, Y. Yan, M. Ahmed, H. Yamashita, J. I. Warrick, J. D. Raman, D. J. DeGraff and P. K. Wong, *Cells*, 2021, 10, 3084.
- 25 D. S. Glass, X. Jin and I. H. Riedel-Kruse, *Phys. Rev. Lett.*, 2016, **116**, 128102.
- 26 S. Chigurupati, T. V. Arumugam, T. G. Son, J. D. Lathia, S. Jameel, M. R. Mughal, S.-C. Tang, D.-G. Jo, S. Camandola, M. Giunta, I. Rakova, N. McDonnell, L. Miele, M. P. Mattson and S. Poosala, *PLoS One*, 2007, 2, 1–9.
- 27 M. Boareto, M. K. Jolly, E. Ben-Jacob and J. N. Onuchic, *Proc. Natl. Acad. Sci. U. S. A.*, 2015, 112, E3836–E3844.
- 28 T.-Y. Kang, F. Bocci, M. K. Jolly, H. Levine, J. N. Onuchic and A. Levchenko, *Proc. Natl. Acad. Sci. U. S. A.*, 2019, **116**, 23551–23561.
- 29 M. C. Cross and P. C. Hohenberg, Rev. Mod. Phys., 1993, 65, 851–1112.
- 30 O. Barad, D. Rosin, E. Hornstein and N. Barkai, *Sci. Signaling*, 2010, 3, ra51.
- 31 M. Cohen, B. Baum and M. Miodownik, *J. R. Soc., Interface*, 2011, **8**, 787–798.
- 32 M. Galbraith, F. Bocci and J. N. Onuchic, *PLoS Comput. Biol.*, 2022, **18**, 1–26.
- 33 G. J. Podgorski, M. Bansal and N. S. Flann, *Nat. Commun.*, 2007, 4, 1742–4682.
- 34 G. L. Hunter, Z. Hadjivasiliou, H. Bonin, L. He, N. Perrimon, G. Charras and B. Baum, *Development*, 2016, 143, 2305–2310.
- 35 S. Toda, L. R. Blauch, S. K. Y. Tang, L. Morsut and W. A. Lim, *Science*, 2018, **361**, 156–162.
- 36 N. Mulberry and L. Edelstein-Keshet, *Phys. Biol.*, 2020, 17, 066003.
- 37 R. Cohen, L. Amir-Zilberstein, M. Hersch, S. Woland, O. Loza, S. Taiber, F. Matsuzaki, S. Bergmann, K. B. Avraham and D. Sprinzak, *Nat. Commun.*, 2020, **11**, 5137.
- 38 S. Bajpai, R. Prabhakar, R. Chelakkot and M. M. Inamdar, *J. R. Soc., Interface*, 2021, **18**, 20200825.
- 39 S. Bajpai, R. Chelakkot, R. Prabhakar and M. M. Inamdar, *Soft Matter*, 2022, **18**, 3505–3520.
- 40 S. A. Vilchez Mercedes, F. Bocci, H. Levine, J. N. Onuchic, M. K. Jolly and P. K. Wong, *Nat. Rev. Cancer*, 2021, 21, 592–604.
- 41 F. Bocci, M. K. Jolly, J. T. George, H. Levine and J. N. Onuchic, *Oncotarget*, 2018, **9**, 29906.